INVESTIGATION OF MESH SENSITIVITY IN COUPLED THERMAL-HYDROLOGICAL-MECHANICAL MODELS: EXAMPLES FROM DESERT PEAK, NEVADA, USA AND NGATAMARIKI, NEW ZEALAND

S. Kelkar[1], D. Dempsey[1], G. Zyvoloski[2], J. Pogacnik[3],

[1]Los Alamos National Laboratory, Los Alamos, New Mexico, USA

[2]Los Alamos National Laboratory, Retired, gazyvoloski@gmail.com

[3]Department of Engineering Sciences, University of Auckland, Auckland, New Zealand

kelkar@lanl.gov

Keywords: *Geothermal, injectivity, stimulation, numerical model, coupled flow-stress, mesh sensitivity.*

ABSTRACT

Dempsey et al. (this issue) have presented validation of a coupled thermal-hydrological-mechanical model through a comparative study of shear stimulation in geothermal fields at Desert Peak, Nevada, USA and Ngatamariki, New Zealand. Values of model parameters obtained from such validation studies are often used for extrapolating the model results beyond the domain of available experiments. Thus it is important to consider the sensitivity of these results to the specifics of the model setup as well as uncertainties in input parameters. In this presentation, we consider the sensitivity of history-matched parameter values to the numerical meshes on which computations are performed.

During well stimulation, it has been noted that injectivity varies with time according to a power law, i.e., $\boldsymbol{II} \propto \boldsymbol{t^n}$, with $\boldsymbol{n}$ ranging between 0.3 and 0.7. Dempsey et al. propose that $\boldsymbol{n}$ depends on the geometry of the stimulated region. However, this result is dependent on permeability enhanced according to a Mohr-Coulomb failure criterion, which is informed by the stress solution. It is well known that that the finite element method, in linear elastostatics, displays optimal rates of convergence in the L2 norm of stress error with mesh refinement (Zienkiewicz and Taylor, 1994). However, the situation is significantly more complicated in fully-coupled THM modelling. Stress-induced permeability changes affect both the fluid mass balance and energy/enthalpy balance equations and the subsequent convergence of the entire coupled system of equations. Relying on solutions found on an un-converged discretization could result in significant errors. We evaluate this dependence for several grid geometries to establish the robustness of the model findings.

1. INTRODUCTION

High temperature rock formations at moderate depths with low intrinsic permeability are candidates for Enhanced Geothermal Systems (EGS) projects. Hydraulic stimulation can be employed in such systems to create flow paths with low impedance while maintaining significant heat transfer areas to avoid premature cooling of the conductive formation. The stimulation treatments have to be designed and implemented with care to achieve the desired injectivity gain while avoiding the creation of short-circuiting flow paths. This involves complex processes of heat and mass transfer, mechanical deformation and failure, and geochemical considerations, e.g., precipitation and dissolution. EGS relies on mechanical failure of fractured rock formations caused by fluid interaction with fractures including thermal and pressure effects. Rock failure subsequently affects the heat and mass transfer through the enhancement of permeability and fracture surface area. Therefore, one challenge facing the reservoir modelling community is the robust representation of these coupled processes within a single numerical framework.

In recent years, several simulators have emerged that are designed to address such tightly coupled thermo-hydrological-mechanical (THM) processes ((Zyvoloski 2007; Podgorney et al. 2010; Rutqvist & Tsang 2003). However, the absence of simple analytical solutions has made benchmarking these simulators an ongoing challenge. Thus, issues of mesh discretization, time-stepping and convergence are difficult to address.

It is well known that that the finite element method, in linear elastostatics, displays optimal rates of convergence in the L2 norm of stress error with mesh refinement (Zienkiewicz and Taylor, 1994). Also, many studies of numerical grid effects have been presented in the context of fluid flow and contaminant transport (e.g. Zyvoloski & Vesselinov 2006). Similar studies need to be conducted in the field of coupled THM modelling- this work provides a step in that direction. Here the situation is significantly more complicated. Stress-induced permeability changes affect both the fluid mass balance and energy/enthalpy balance equations and the subsequent convergence of the entire coupled system of equations. Relying on solutions found on an un-converged discretization could result in significant errors. We evaluate this dependence for several grid geometries to establish the robustness of the model findings.

In lieu of an analytical solution, we use data from a well-characterized field experiment – the Desert Peak EGS demonstration project – to construct and calibrate a coupled THM model. The measured injectivity of the stimulated well is used as a metric against which to benchmark the performance of the model. Specifically, we investigate the robustness of a particular calibration with regard to mesh discretization. Our principal findings are that: (i) the calibrated permeability decreases at higher mesh discretization due to decreasing control volume area; (ii) for larger grid blocks, fracture failure parameters, e.g., friction and cohesion, must be varied to offset the increased thermal mass and resistance to thermally induced failure; and (iii) it may not always be advisable to use physically correct parameter values on coarsely discretized meshes. This investigation is extended to a well stimulation at the Ngatamariki geothermal field, New Zealand, to verify the generality of these findings.

2. BENCHMARK DATASETS

Stimulation of a geothermal well is a useful benchmark problem due to the tight coupling between stress, heat transfer and fluid flow. However, construction of a robust numerical model that represents a given stimulation requires (i) a comprehensive characterization of the site's thermal and elastic parameters, its intrinsic fracture properties and their response to stressing, and the initial state of the reservoir, i.e., the model inputs; and (ii) high-quality monitoring of the response of the system to stimulation, e.g., injectivity, mass flow rates, down-hole pressure and temperature conditions with time, i.e., the outputs. These data are available to varying quality for the two EGS stimulations considered here – Desert Peak, Nevada and Ngatamariki, New Zealand. Site and stimulation overviews are supplied below.

2.1 Desert Peak, Nevada, USA

Desert Peak is a high-enthalpy, blind geothermal system associated with NE-striking normal-faulting in western Nevada (Fig. 1). Hydraulic fracturing tests in the stimulated well indicate the magnitude of σ_h is ~0.61 of the overburden stress, σ_v (Hickman and Davatzes, 2010). Wellbore imaging and core testing indicated the stimulation interval was a moderately porous, siliceous rhyolite containing in-situ fractures with limited structural anisotropy. Temperatures of 190-210°C were encountered at the stimulation depth of 920 to 1070 m and initial formation pressure is assumed hydrostatic below a water table 116 m below the ground surface.

Beginning in September 2010, cold water was injected at four increasing pressure steps. In order to avoid hydraulic fracturing, the applied wellhead pressures (WHPs), 1.5, 2.2, 3.1 and 3.7 MPa, were specifically restricted to be less than the minimum principal stress, σ_h. The majority of the injectivity improvement took place during the 45-day 3.1 MPa pressure step. Injectivity began to increase ~6 days after injection began, starting at 0.15 and eventually reaching 1.5 kg s^{-1} MPa^{-1}. The injectivity curve is approximately linear under-log transformation; a straight-line fit to the data suggest the exponent of injectivity evolution, n, is between 0.3 and 0.4 (Dempsey et al., this issue).

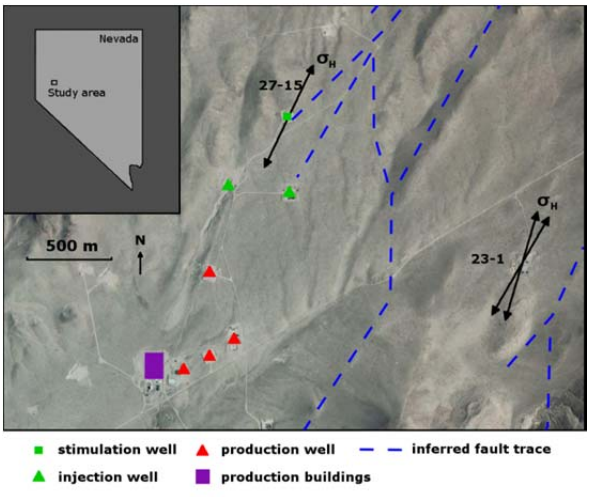

Figure 1: Summary of infrastructure, inferred structures and stress state at Desert Peak geothermal field (from Dempsey et al., 2013). Stimulation took place at well 27-15.

2.2 Ngatamariki, NZ

Ngatamariki Geothermal Field is in the North Island, New Zealand; located in the Taupo Volcanic Zone (TVZ), a region of active rifting, normal faulting and robust rhyolitic Quaternary volcanism. The maximum horizontal principal stress at Ngatamariki is approximately aligned with the strike of faulting (σ_H = 30↔210°) and a high-degree of fracture orientation anisotropy is reported.

In 2011-2013, one producer and three deep injection wells were drilled in the field. After completion testing, the injection wells were injected with 20°C river water for periods of 19 to 31 days to improve well injectivity. The rate of stimulation of one such well was quantified and reported in Grant et al. (2013). .

During the 30-day stimulation, injectivity increased from an initial value of ~1 to between 7 and 8 kg s^{-1} MPa^{-1}. Thus, initial and final injectivity are about an order of magnitude higher than at Desert Peak. Furthermore, injectivity gains were more-immediate, being observed after only one day of injection. Log-analysis of the data also suggests that the injectivity exponent for this stimulation is higher (~0.6, Grant et al., 2013).

Due to limitations on data availability, characterization of formation properties and initial reservoir state is less comprehensive for the Ngatamariki site. Nevertheless, the dataset is useful for assessing whether the specific sensitivities illustrated by the Desert Peak model have more general application.

3. NUMERICAL MODEL

3.1 Computational Code

Stimulation is modelled using the code Finite Element Heat and Mass transfer (FEHM) developed at Los Alamos National Laboratory, originally developed to model non-isothermal fluid flow in geothermal reservoirs (Zyvoloski, 2007) and extended to coupled stress applications (Kelkar et al. 2012). FEHM is an integrated code capable of solving fully coupled nonlinear continuum equations of mass balance, heat transfer, and mechanical deformations in fractured porous media. Newton-Raphson outer iterations are used with a complete Jacobian and efficient linear equation solvers. FEHM has been developed extensively under projects on conventional/unconventional energy extraction (geothermal, oil, and gas), radionuclide and contaminant transport, watershed management, and CO_2 sequestration. FEHM solves continuum equations for porous flow, heat transfer, and deformation using a combination of control volume and finite element approaches. FEHM's capabilities include non-isothermal, multiphase, multi-component fluid flow, heat transfer and chemical transport in media with dual porosity, dual permeability on unstructured grids. FEHM uses an efficient approach for evaluating thermodynamic functions using lookup tables and polynomial approximations to calculate derivatives in the finite element computations. FEHM also uses a novel technique of uncoupling the material coefficients from the geometric integrals involving shape functions. This allows us to pre-compute the geometric integrals at the beginning of the simulation, saving significant computational resources during iterative solutions of nonlinear problems.

We discretize the mass and energy balance equations (TH) using the control volume (CV) approach, as this is known to lead to good local mass conservation (Versteeg and

Malalasekera [2007]). The mechanical force balance equations (M) are discretized with the finite element (FE) approach. The reason for this choice is that FE stresses calculated at the Gauss points are known to be of higher order accuracy than average stresses calculated at the nodes (Zienkiewicz and Taylor, 1994). This is important for the applications considered here as there is a strong coupling between the TH and the M equations (for example, the permeability can increase by many order of magnitude upon material failure), and failure criteria such as Mohr-Coulomb, Von Mises or Drucker-Prager (e.g., Jaeger and Cook [1997]) depend on the state of stress rather than the displacements. The work presented here uses 8-noded hexahedral iso-parametric elements with linear shape functions having C_0 continuity. The same set of nodes is used for both the CV and the FE formulations – the correspondence between the two is shown in Figure 2.

The mass balance equations using the control volume approach need effective permeabilities at interfaces between connected pairs of nodes, which are commonly computed from the nodal values using harmonic averaging to conserve mass. We apply a mechanical factor determined as a function of stress to the permeabilities at each node. The stresses at each node are calculated as the averages over all the elements connected to that node.

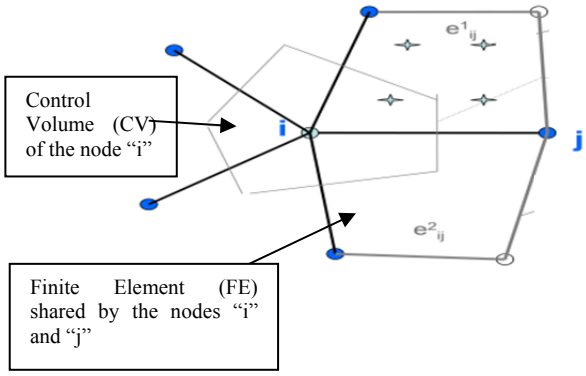

Figure 2. A schematic representation of the mapping between control volume and finite element.

3.2 Stress-permeability relationship

This model has been presented in detail by Dempsey et al. (this issue), and only a brief description is given here for completeness. Two somewhat different models were used for the two field cases considered here – Desert Peak and Ngatamariki- although they both incorporated the Mohr-Coulomb failure criteria and modifications to permeability based on the damage due to failure.

The conceptual model used to match the Desert Peak data is of an ensemble of pre-existing fractures, each of which fully transects the control volume. A set of N such fractures, each with an orientation picked from a prescribed distribution, are assigned to each control volume, and the permeability at the node is taken to be an ensemble average over the N fractures. The permeability of each fracture depends on a calculated stress drop assuming Mohr-Coulomb failure and static/dynamic friction behaviour (McGarr, 1999). The stress drop parameter is similar to that used to calculate earthquake magnitudes. Stress drop across the fracture is related to a shear displacement through the shear stiffness of the fracture. Permeability enhancement is then calculated with respect to shear displacement on the fracture in accordance with empirical relationships established by laboratory sliding experiments (Lee and Cho, 2002).

For the case of the Ngatamariki field, the permeability relationship described above is modified, as justified by Dempsey et al. (this issue) so that only a single fracture is assigned to each control volume. The fracture normal is oriented parallel to σ_h - this provides the best accuracy in terms of resolving permeability anisotropy on a Cartesian mesh. The shear failure criterion is still assessed for this fracture orientation; however, user specified permeability multipliers are used parallel and perpendicular to the fracture – this provides control of the stimulation geometry.

3.3 Model setup

The computational domain is 4km x 4km x 2km (fig. 3) centred on the injection interval with increasing resolution closer to the centre. The highest resolution extends 30 m out from the injection node which is sufficient to capture the extent of the damage region formed during the 45-day stimulation. The injection source is specified as a fixed overpressure, corresponding to the applied WHP, e.g., 3.1 MPa for the Desert Peak model. Modelled mass flow is then proportional to the pressure difference between the well and the reservoir. Injectivity index is defined as flow rate, Q, divided by the pressure difference in the well, P_{DHP}, and the formation, P_{RES}, i.e., $II = Q/(P_{DHP} - P_{RES})$. In this work, the applied WHP is taken as a proxy for the pressure difference. During stimulation, the injected flow rate increases despite a fixed WHP; this indicates induced changes in rock permeability.

Fixed pressure and no heat flux boundary conditions are applied at all boundaries. The Desert Peak model was initialized with hydrostatic pressure and temperatures consistent with pre-stimulation conditions, i.e., 190-210°C. Vertical gradients in the principal stress components are applied as an initial condition. The Cartesian axes are chosen to align with the principal stresses, i.e., $\sigma_x, \sigma_y, \sigma_z = \sigma_h, \sigma_H, \sigma_v$; this reduces the magnitude of off-diagonal permeability components that cannot be represented in the model. The vertical stress is given by the overburden, while the minimum principal (horizontal) stress gradient is specified as a fractions of the vertical; for Desert Peak, this was determined by a hydraulic fracturing test in the well to be σ_h=0.61σ_v (Hickman and Davatzes, 2010). The median principal stress (horizontal) was taken to be the mean of the maximum and the minimum. Water was injected at 100°C at a depth of 1000 m. Permeability is enhanced as a function of induced stresses as outlined in Dempsey et al. (2013). Model parameters are summarized in Table 1.

Table 1. Base case parameters for numerical model to match the Desert Peak data.

Parameter	Value
Operational	
Injection depth	1000 m
Injection pressure	3.1 MPa
Injection temperature[1]	100°C
Material	
Thermal conductivity	2.2 W m^{-1} K^{-1}
Density	2480 kg m^{-3}
Specific heat capacity	1200 J m^{-3} K^{-1}

Porosity	0.1
Coefficient thermal expansion	3.5×10^{-5} K^{-1}
Young's modulus	25 GPa
Poisson's ratio	0.2
Reservoir	
Reservoir temperature	190°C
Initial permeability $[X, Y, Z]$	see table 2
Fracture	
Fractures per control volume, N	100
Max permeability multiplier	*see table* 2
Cohesion, S_0	see table 2
Static friction coef., μ_s	0.65
Dynamic friction coef., μ_d	0.55
Shear fracture stiffness, K_s	5×10^2 MPa m^{-1}

[1]Injection temperature was estimated from a Temperature/Pressure/Spinner-Flow meter log collected after the 3.1 MPa stimulation.

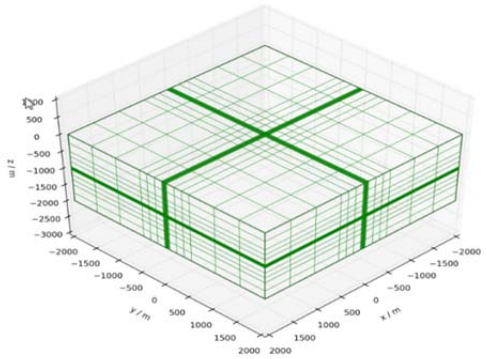

Figure 3. Computational grid used for modelling Desert Peak and Ngatamariki injectivity data.

In general, model calibration against the available injectivity data proceeded as follows: (i) initial reservoir permeability was adjusted to match the initial injected flow rate for the fixed WHP; (ii) fracture cohesion was adjusted to match the onset time of injectivity gain; (iii) limiting fracture permeability was adjusted to match the magnitude of injectivity gain; (iv) in some cases the coefficients of friction were adjusted to match the slope of the flow rate vs. time data. Calibrated values of initial permeability, cohesion, and permeability gain, along with other material properties are given in Table 1.

The Ngatamariki model is a modified version of the Desert Peak model, as described in Dempsey et al. (this issue). The primary differences between the two models are (i) a higher initial permeability in order to capture the higher initial injectivity, and (ii) a greater degree of anisotropy in the geometry of the stimulated region.

4. SENSITIVITY TO SPATIAL DISCRETIZATION

4.1 Desert Peak

Table 2 shows the values of adjusted parameters needed to obtain a reasonable fit to the field data from Desert Peak well 27-15. The fit to the data was obtained visually; parameter estimation programs were not used. Base case match between the calibrated Desert Peak model with a grid spacing of 2m near the injection point and the corresponding injectivity measurements are shown in Fig 4a.The modelled injectivity evolution fits the data moderately well, particularly at early times.

Table 2. Parameter values required to match the Desert Peak flow rate data for various grid spacings, dx. kx_0 = initial permeability, dk_{mult} = permeability multiplier, S_0 = cohesion, μ_s/μ_d = static/dynamic friction coefficients, n = injectivity evolution exponent.

dx (m)	kx_0, kz_0 ky_0 (m^2)	dk_{mult} (log10)	S_0 (MPa)	μ_s/μ_d	n
2	18. x 10^{-16} 90. x 10^{-16}	1.35	11.3	0.75/ 0.65	0.39
5	3.5 x 10^{-16} 1.7 x 10^{-16}	2.2	1.5	0.65/ 0.55	0.41
7.5	2.5 x 10^{-16} 12.5 x 10^{-16}	2.7	0.5	0.65/ 0.55	0.63
10	1.5 x 10^{-16} 7.5 x 10^{-16}	4.5	0.01	0.65/ 0.55	0.58

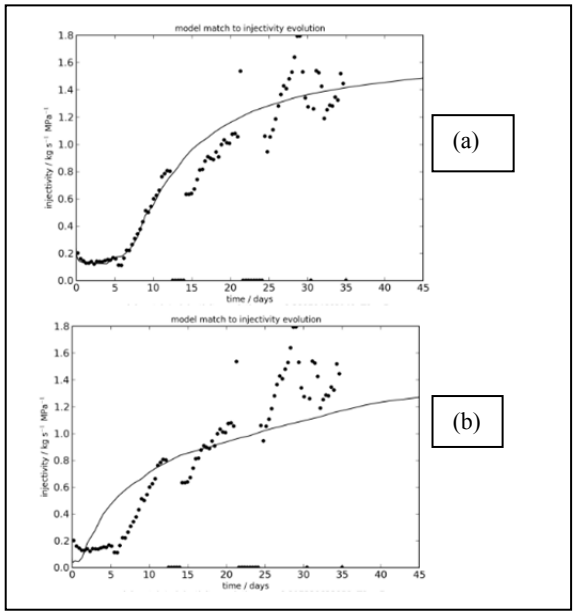

Figure 4. (a) Match to the Desert Peak injectivity data (black dots) as a function of time with a model (black line) using grid spacing of 2m; (b) model results using 2m grid spacing but parameter values calibrated for a 5m grid spacing.

Figure 4b shows the model results using the 2m grid spacing, but using the parameter values obtained from the 5m grid. It is seen that the fit to the data is quite poor, demonstrating the need for recalibrating the parameters when changing the grid spacing. This recalibration generally involves two or three steps.

First, for the case where grid-spacing is refined, the modelled flow rate generally drops. Thus, permeability is increased until a good match is once more obtained. The unstimulated injection rate is sensitive to grid-spacing because the source term is specified via a fixed flowing pressure. After calibrating for flow rate, the second step is to capture the injectivity onset time. In the case of Desert Peak, this is six to seven days after the beginning of the 3.1 MPa stimulation. Injectivity onset reflects the extent to which stresses are perturbed before damage starts to occur and is sensitive to several parameters including thermal mass, coefficient of thermal expansion, Young's modulus, Mohr-Coulomb failure parameters of rock friction and cohesion. In

this work, for the sake of simplicity, we adjusted the value of cohesion to obtain a match to the data, although other parameters could have been adjusted as well.

Convergence considerations (e.g., Zienkiewicz and Taylor, 1994) would indicate that the parameter values corresponding to the smallest grid size used, 2m here, would be closest to the physical values. However, it would be incorrect to use those values when employing a coarser grid, such as may be necessary for computations extrapolating to longer time scales. A more realistic approach might be to calibrate the coarse grid model to the short time data and use those parameter values, even though they may be physically less reasonable.

There is a systematic trend seen in Table 2 with respect to the initial permeability, values decreasing as the grid spacing grows. This can be understood by recalling that these simulations are performed by applying specified pressures at the injection node. As the grid spacing grows so does the inter-nodal cross-sectional area available for flow, and this more than compensates for the lower computed pressure gradient on a coarser mesh. Thus the computed flow rate increases. Hence, to keep the computed flow rate at the value measured in the field, the value of permeability used in the model must be decreased.

The permeability multiplier needed to match the later-time data increases with the increasing grid spacing- a large value of 4.5 on the log-10 scale is required for the 10m grid spacing. This value is not to be interpreted as a physically realistic value, but rather as an input to the numerical model to obtain a reasonable fit to the data. This suggests that caution should be used when interpreting the model results when using large grid spacing.

In Table 2 there is also a trend for cohesion decreasing from 11.3 MPa at 2m spacing to nearly 0 at 10m spacing. An explanation for this is that at a specified injection pressure, the reduction in the normal stress on a fracture is driven by thermal cooling of the block. As the grid spacing grows, so does the thermal mass of the grid block, slowing down the thermally induced reduction in the normal stress. In the case of the 10 m block, where calibrated cohesion is nearly zero, the initial delay before the onset of injectivity improvement is entirely due to the increased thermal mass of the block itself.

Consistent with the observations of Grant et al. (2013), a generally linear relationship persists for the time evolution for each grid sizes explored here. The computed values of the injectivity index n are also reported in Table 2. Although there is no clear trend, a general observation from the table is that the finer grids have a lower n value. Dempsey et al. (this issue) note a connection between the geometry of the damage zone and the injectivity index; lower values of n correspond to a more spherical geometry of the stimulated region. Figure 5a and 5b show respectively the shape of the temperature contours after 45 days of pumping for grids with 2m and 10 m spacing respectively. Clearly the shape of the cooled region is more spherical for the 2m case compared to the 10m case; this is consistent with the findings of Dempsey et al. (this issue).

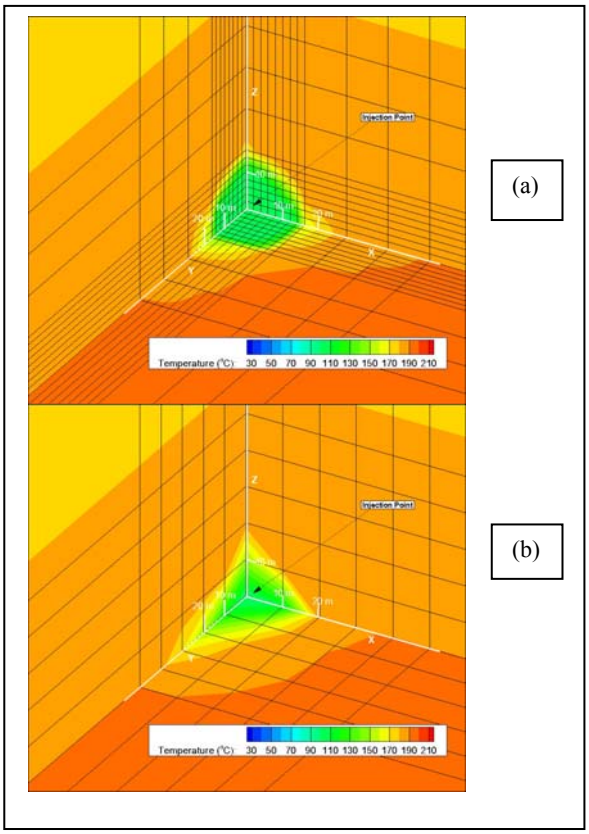

Figure 5. A cut-away through the injection point showing temperature contours after 45 days of injection for (a) 2m grid spacing (b) 10 m grid spacing.

Increased anisotropy in the coarser grid results from a subtle interaction between a near-critical stress state, poor resolution of sharp stress gradients, and inadequate representation of injection zone plasticity. As the rock near the injection well cools, it contracts; in response, warmer rock in the vicinity expands into the void created. Depending on the relative location, this expansion can be coincident with the ambient extensional stresses and therefore result in failure. Generally, this effect is small and occurs over a short distance; however, at lower resolution, it is more extensive and introduces an artificial source of anisotropy. Furthermore, it is exacerbated by unrealistic tensional stress states that occur near the injection well. In future models, an elastoplastic formulation will be applied to limit these injection-induced stresses.

4.2 Ngatamariki

Three different grid spacings in the vicinity of the injection point were considered for the Ngatamariki data: 2m, 3m, and 4m. Model calibration was done in a manner similar to that described in Section 4.2.1 for the Desert Peak data; except that the cohesion was kept near zero (0.01 MPa) for all cases. Despite this choice, the model predicted a somewhat delayed injectivity rise compared to the data. As Dempsey et al. (this issue) have discussed, this could be due to the extreme anisotropy that may be present at the Ngatamariki field. Since the model match to the data was not very good at early time, we did not adjust the initial permeability values for different grids. However the permeability multipliers were adjusted to get a good match for the later time data. Figures 6a, 6b, 6c show the match for grid spacings of 2, 3, and 4 m respectively. The values show

trends with respect to the grid spacing similar to those discussed for the Desert Peak model in the previous section.

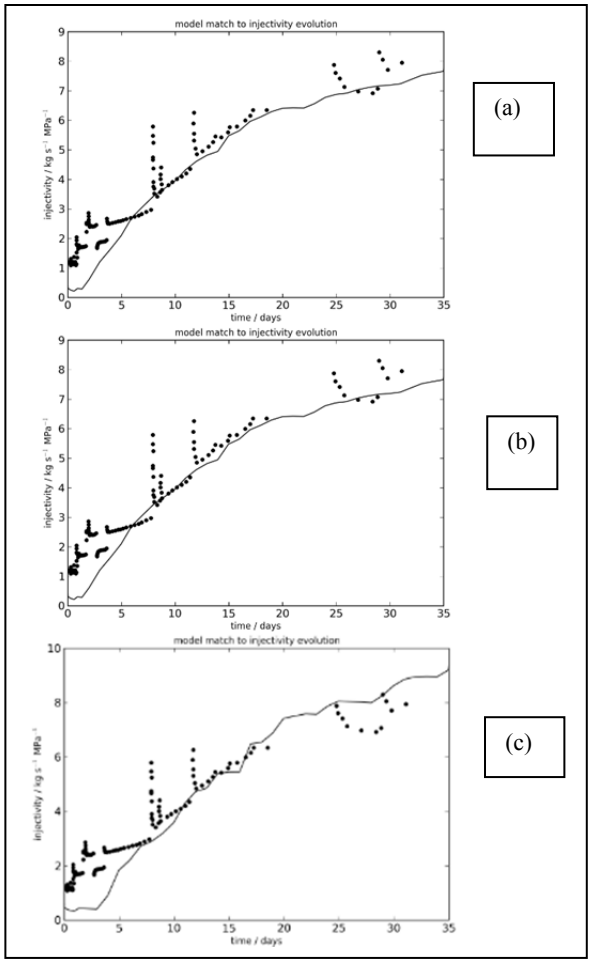

Figure 6.Match to Ngatamariki injectivity data (black dots) with the model results (black line) (a) 2m grid spacing (b) 3m grid spacing, and (c) 4m grid sapcing

5. CONCLUSION

We have presented the results of a coupled THM model, based on the code FEHM, including stress dependant permeability variations upon shear failure on existing fractures. Using various grid spacings, we have matched the data from a well-characterized field experiment – the Desert Peak (Nevada, USA) EGS demonstration. The measured injectivity of the stimulated well is used as a metric against which to benchmark the performance of the model. We have presented similar modelling results to match the data from another field- Ngatamariki (North Island, New Zealand). Our principal findings are that: (i) the calibrated permeability decreases at higher mesh discretization; (ii) for larger grid blocks, fracture failure parameters, e.g., friction, cohesion, need to be varied to offset the increased thermal mass and resistance to thermally induced failure; and (iii if coarsely discretized meshes cannot be avoided, then it is advisable to use parameter values calibrated to give a good match to the data, even if these are not strictly physically correct.

ACKNOWLEDGEMENTS

Funding for this work was provided by US DOE Office of Geothermal Technologies under Work Authorization No. GT-100036-12_Revision 1. The coupled flow and stress numerical simulation capabilities in FEHM applied for this work were developed at LANL under the Zero Emission Research & Technology (ZERT-II) project funded by US DOE through its CO_2 sequestration R&D program.

REFERENCES

Dempsey, D., Kelkar, S., Lewis, K., Hickman, S., Davatzes, N., Moos, D., Zemach, E., (2013). Modeling Shear Stimulation of the Desert Peak EGS Well 27-15 Using a Coupled Thermal-Hydrological-Mechanical Simulator. *Proc. 47th US Rock Mech. Symp.*

Dempsey, D., Clearwater, J., Kelkar, S., Wallis, I., *This issue*. Validation of a Coupled Thermal-Hydrological-Mechanical Model Through a Comparative Study of Shear Stimulation in Two Geothermal Environments: USA and New Zealand.

Grant, M, A., Clearwater, J., Quinao, J., Bixley, P. F., Le Brun, M., (2013). Thermal Stimulation of Geothermal Wells: A Review of Field Data. *Proc. 38th Stanford Geotherm. Workshop*.

Hickman, S. H., Davatzes, N. C., (2010). In-situ Stress and Fracture Characterization For Planning of an EGS Stimulation in the Desert Peak Geothermal Field, Nevada. *Proc.* 35th Stanford Geotherm. Workshop.

Jaeger, J., Cook, N., 1997. Fundamentals of Rock Mechanics, 3rd Edition. Chapman and Hall Ltd., New York, NY, USA.

Kelkar S, Lewis K, Hickman S, Davatzes N, and Moos D., (2012) Modeling coupled thermal-hydrological-mechanical processes during shear stimulation of an EGS well. Presented at the Thirty-Seventh Workshop on Geothermal Reservoir Engineering, Stanford University, Stanford, California, January 30-February 1, 2012.

Lee, H. S., Cho., T. F., (2002). Hydraulic Characteristics of Rough Fractures in Linear Flow under Normal and Shear Load. *Rock Mech. Rock Engng.* v. 35, pp. 299-318.

Lutz, S. J., Hickman, S. H., Davatzes, N. C., Zemach, E., Drakos, P., Robertson-Tait, A, (2010). Rock Mechanical Testing and Petrologic Analysis in Support of Well Stimulation Activities at the Desert Peak Geothermal Field, Nevada, *Proc. 35th Stanford Geotherm. Workshop.*

McGarr, A., (1999). On relating apparent stress to the stress causing earthquake fault slip. *J. Geophys. Res.*, v. 104, pp. 3003-3011.

Podgorney, R., Huang, H., Gaston, D. (2010). Massively parallel fully coupled implicit modeling of coupled thermal- hydrological-mechanical processes for enhanced geothermal system reservoirs. In: Proceedings 35th Workshop on Geothermal Reservoir Engineering, Stanford University, Stanford, CA.

Rutqvist, J., Tsang, C., (2003). TOUGH-FLAC: a numerical simulator for analysis of coupled thermal-hydrologic-mechanical processes in fractured and porous geological media under multi-phase ow conditions. In: Proceedings of the TOUGH Symposium. pp. 12{14.

Versteeg, H., & Malalasekera, W., (2007). An introduction to computational fluid dynamics: the finite volume method. Prentice Hall.

Zienkiewicz D.C. & Taylor R.L. (1994), "The Finite Element Method, Fourth Edition, Vol 1: Basic Formulations and Linear Problems" McGraw Hill Book Company, 1994, pp 398-407.

Zyvoloski, G.A. & Vesselinov, V.V., (2006). An Investigation of Numerical Grid Effects in Parameter Estimation. Groundwater, Vol. 44, No. 6, pp 814-825.

Zyvoloski, G. A.: FEHM: A control volume finite element code for simulating subsurface multi-phase multi-fluid heat and mass transfer. *LANL Doc. LAUR-07-3359*. Los Alamos, NM. (2007)